

# Subthalamic nucleus stimulation reverses mediofrontal influence over decision threshold

James F Cavanagh<sup>1</sup>, Thomas V Wiecki<sup>1</sup>, Michael X Cohen<sup>2,3</sup>, Christina M Figueroa<sup>1</sup>, Johan Samanta<sup>4,5</sup>, Scott J Sherman<sup>4</sup> & Michael J Frank<sup>1,6,7</sup>

It takes effort and time to tame one's impulses. Although medial prefrontal cortex (mPFC) is broadly implicated in effortful control over behavior, the subthalamic nucleus (STN) is specifically thought to contribute by acting as a brake on cortico-striatal function during decision conflict, buying time until the right decision can be made. Using the drift diffusion model of decision making, we found that trial-to-trial increases in mPFC activity (EEG theta power, 4–8 Hz) were related to an increased threshold for evidence accumulation (decision threshold) as a function of conflict. Deep brain stimulation of the STN in individuals with Parkinson's disease reversed this relationship, resulting in impulsive choice. In addition, intracranial recordings of the STN area revealed increased activity (2.5–5 Hz) during these same high-conflict decisions. Activity in these slow frequency bands may reflect a neural substrate for cortico-basal ganglia communication regulating decision processes.

It is widely believed that the prefrontal cortex (PFC) facilitates deliberative control over behavior<sup>1,2</sup>, but many of the mechanistic details of this influence remain to be defined. Here we describe how a PFC-basal ganglia system implements slower, more controlled decisions during difficult choices. The mPFC has been proposed to instantiate control over behavior based on an evaluation of endogenous or exogenous conflict<sup>3,4</sup>. When control is needed, the mPFC communicates with the STN of the basal ganglia, which acts as a brake on the cortico-striatal system to facilitate a more deliberative response process<sup>5,6</sup>. The STN receives direct projections from the mPFC, forming a 'hyperdirect' pathway that can rapidly modulate cortico-striatal processing<sup>6–9</sup>. This architecture makes the STN ideally suited to receive input from, and ultimately influence, processing of action selection in mPFC.

Theories of cortico-basal ganglia functioning predict an interaction between mPFC and the STN in the online regulation of behavior, particularly when habitual responses are overridden to make planned and controlled responses. Although the mPFC is involved in both the facilitation and inhibition of candidate motor actions, the STN is thought to primarily inhibit the prepotent action<sup>10,11</sup>. According to this framework, mPFC-STN communication serves to exert control in conditions in which cortico-striatal signaling would induce impulsive responding. Although evidence supports this idea of a hyperdirect pathway, much of it remains correlational (functional magnetic resonance imaging, white matter tractography and nonhuman primate electrophysiology)<sup>7,10–13</sup>.

Disrupting STN function through high-frequency deep brain stimulation (DBS) is an increasingly common treatment for Parkinson's disease, providing an opportunity to manipulate the STN area

while monitoring control over decisions and actions. As might be expected, DBS can induce impulsivity in affected individuals' day-to-day lives<sup>14</sup>, and this effect can be captured in the laboratory. A previous study reported that STN-DBS disrupted the tendency to adaptively slow down when faced with difficult decisions<sup>15</sup>. On the basis of computational modeling of basal ganglia function in decision making, it was proposed that the mPFC influences processing in STN to modulate the decision threshold during response conflict<sup>5</sup>, and that DBS interferes with this function, thereby leading to impulsivity. Crucially, this abstract measure of decision threshold can be inferred from computational modeling of response time distributions<sup>16</sup>. This model-based approach helps to parse variance between multiple latent processes that have been suggested to be reflected in accuracy and response time. As yet, however, there are no empirical data that demonstrate such mPFC-STN interactions during conflict.

Electroencephalography (EEG) is commonly used to assess mPFC activities during conflict and control<sup>3,4</sup>. Specifically, theta-band power over the mPFC increases following punishment, error or conflict, and the degree of theta power increase predicts subsequent response time slowing, suggesting a direct role in adaptive control<sup>17–19</sup>. Thus, this EEG feature is a promising candidate for measuring the influence of mPFC on conflict-related threshold adjustment while manipulating the effective functioning of the STN area via DBS (see **Fig. 1a**).

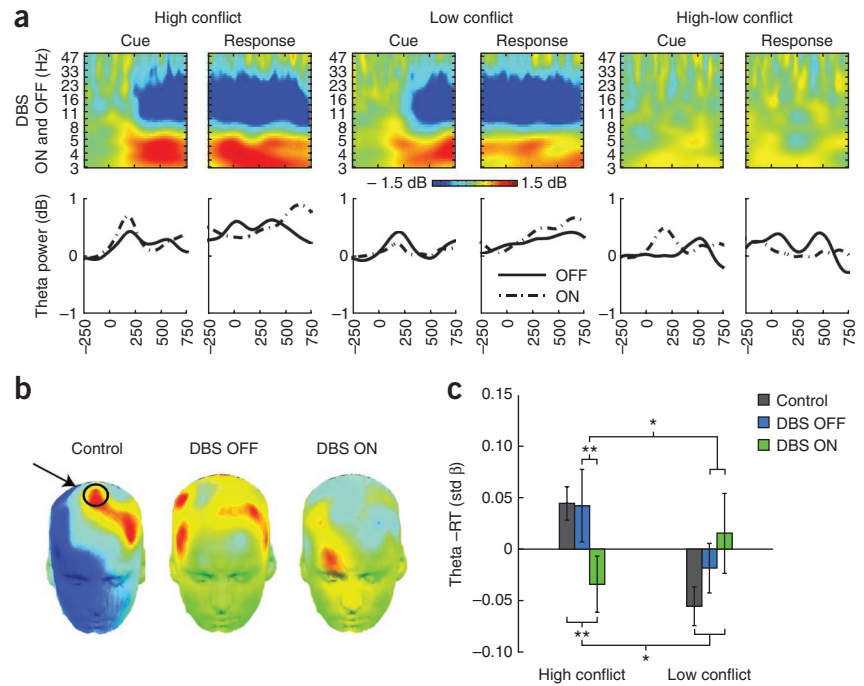
Here we present evidence from two separate studies in which we manipulated or directly measured activity in the STN area. Healthy participants and individuals with Parkinson's disease performed a reinforcement learning and choice conflict task while concurrent EEG was recorded. Affected individuals were tested twice, alternating

<sup>1</sup>Department of Cognitive, Linguistic and Psychological Sciences, Brown University, Providence, Rhode Island, USA. <sup>2</sup>Department of Psychology, University of Amsterdam, Amsterdam, The Netherlands. <sup>3</sup>Department of Physiology, University of Arizona, Tucson, Arizona, USA. <sup>4</sup>Department of Neurology, University of Arizona, Tucson, Arizona, USA. <sup>5</sup>Banner Good Samaritan Medical Center, Phoenix, Arizona, USA. <sup>6</sup>Department of Psychiatry, Brown University, Providence, Rhode Island, USA. <sup>7</sup>Brown Institute for Brain Science, Providence, Rhode Island, USA. Correspondence should be addressed to J.F.C. (jim.f.cav@gmail.com) or M.J.F. (michael\_frank@brown.edu).

Received 7 June; accepted 2 August; published online 25 September 2011; doi:10.1038/nn.2925



**Figure 2** DBS ON/OFF study: scalp EEG (FCz electrode) from the test phase split by high and low conflict. (a) Stimulus presentation and response commission were characterized by notable beta power suppression and theta power enhancement compared with baseline in both ON and OFF conditions, which were combined here. (b) Topoplots of the high-low conflict difference in standardized regression ( $\beta$ ) weights for cue-locked theta power and response time ( $\pm 0.1$  std  $\beta$ ). The FCz site is indicated on the control topoplot. (c) Standardized regression ( $\beta$ ) weights (mean  $\pm$  s.e.m.) for cue-locked theta power and response time, demonstrating that DBS reversed a natural coupling of theta band power with response time slowing on high-conflict trials.



contrasts revealed a difference between DBS conditions during high conflict ( $P = 0.006$ ). There was no difference between high-conflict valence conditions (win-win versus lose-lose) or when the EEG data was time-locked to the response (**Supplementary Figs. 1 and 2**). To determine whether the brain-behavior patterns seen in OFF DBS sessions are natural features of human cognitive architecture and not specific to individuals with Parkinson's disease, we explicitly compared the theta–response time relationships between healthy participants and affected individuals in ON and OFF DBS sessions (**Supplementary Results and Supplementary Fig. 3**). Notably, controls did not differ from affected individuals in OFF DBS sessions in their relationship between mPFC theta and response time adjustment (interaction,  $P = 0.91$ ; high-conflict contrast,  $P = 0.52$ ). In contrast, in ON DBS sessions, this relationship was significantly different from controls (interaction,  $F_{1,77} = 6.38$ ,  $P = 0.014$ ), with a significant contrast for high conflict ( $P = 0.013$ ). In summary, cue-locked high-conflict mPFC theta power predicted an increase in response time; STN-DBS abolished this adaptive slowing and actually revealed an inverse mPFC–response time relationship. These patterns can be accounted for using a computational model of action selection.

### Study 1: drift diffusion modeling

Given these EEG and conflict effects on response times, we sought to determine whether the combined pattern of behavioral results could be accounted for by the hypothesized role of mPFC–STN interactions on conflict-related adjustments in decision threshold. To this end, we fit participants' choices with the drift diffusion model (DDM)<sup>16</sup>, the most widely used mathematical model of two-alternative forced-choice decision-making tasks. DDM can simultaneously account for the proportion of correct and error trials (or optimal and suboptimal trials here) and the full response time distributions for these trials in each task condition. In this framework, behavioral response time distributions are considered to be observations that arise as a function of underlying latent parameters of a decision-making model. Core parameters include the rate of evidence accumulation (drift rate), decision threshold and non-decision time (capturing stimulus encoding and motor execution). Our neural models suggest that, on stimulus presentation, the mPFC first generates candidate actions as a function of their prior probabilities of execution given the stimulus. When there is response conflict (reflected by similar levels of activation between alternative cortical responses), the mPFC–STN network increases the decision threshold, buying more time for the corticostriatal network to evaluate and compare their reward values.

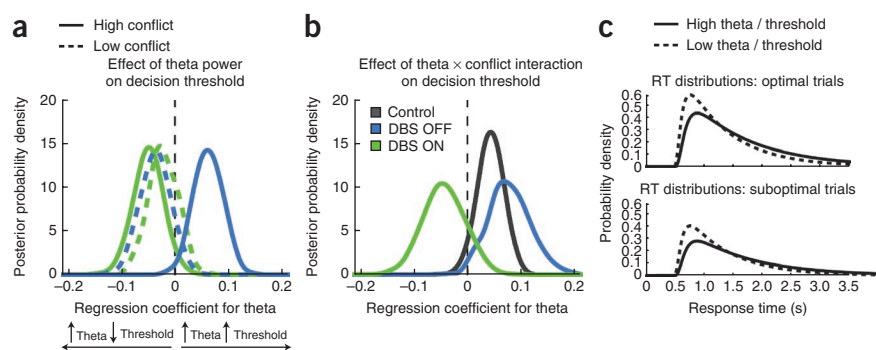
This leads to slower, more dispersed response time distributions and, critically, a relatively lower proportion of fast errors.

To test this hypothesis, we employed hierarchical Bayesian parameter estimation, which deduces the posterior probability density of the diffusion model parameters generating the observed data for the entire group of participants simultaneously, while allowing for individual differences (see Online Methods). We estimated regression coefficients to determine the relationship between trial-to-trial variations in mPFC theta power and decision threshold in low- and high-conflict trials, and whether any such relationship interacted with DBS status.

For affected individuals in OFF DBS sessions, decision threshold in high-conflict trials increased in proportion to the degree of mPFC theta in those trials ( $P = 0.01$ ; **Fig. 3a**). This effect was not present in low-conflict trials ( $P = 0.11$ ). Notably, this effect of theta on high-conflict decision threshold was reversed when DBS was turned ON ( $P = 0.045$ ), yet again there was no effect on low-conflict trials ( $P = 0.23$ ). This influence of DBS state on the correlation between mPFC theta-band power and decision threshold under high conflict was confirmed by a critical DBS  $\times$  theta interaction under high conflict ( $P = 0.001$ ), but not low conflict ( $P = 0.39$ ). These effects of theta and DBS on decision threshold were found even after controlling for drift rate effects on trial type. Moreover, the data cannot be explained by assuming that frontal theta modulates drift rate (which would also alter mean response times, but have different effects on their distributions and error rates), demonstrating the specificity of mPFC theta and STN-DBS in altering the latent decision threshold parameter (see **Supplementary Results and Supplementary Tables 1–3**).

The relationship between mPFC theta and threshold preferentially applied to high-conflict relative to low-conflict decisions (theta  $\times$  conflict interaction; **Fig. 3b**). A positive interaction indicated that the effect of mPFC on decision threshold was greater for high-conflict relative to low-conflict trials. This positive interaction was significant in both the control group ( $P = 0.04$ ) and in affected individuals in OFF DBS sessions ( $P = 0.02$ ). Moreover, although control and affected individuals in OFF DBS sessions did not differ in the effects

**Figure 3** DBS ON/OFF study: Bayesian posterior densities of decision thresholds estimated from the drift diffusion model (ordinates) and how they varied as a function of mPFC theta (abscissa). Peaks of the distributions reflect the most likely value of the parameter. Significance was assessed by at least 95% of the distribution being to the left or right of zero. (a) Simple effects of theta. OFF DBS, increased theta was associated with increased decision threshold for high-conflict trials, but not low-conflict trials. ON DBS, increased theta was associated with a decreased decision threshold on high-conflict trials, but not low-conflict trials. (b) Theta  $\times$  conflict interaction. Increases in theta resulting from high > low conflict were associated with increases in threshold OFF DBS and in healthy controls. The opposite pattern was seen ON DBS. (c) These threshold effects are reflected by changes in response time distributions. These plots show the best fit response time distributions for optimal and suboptimal choices as a function of low and high mPFC theta/threshold in affected individuals in OFF DBS sessions. Higher theta power is associated with a reduction in the density of fast suboptimal choices and greater dispersion of optimal response time distributions, fitting with an account of increased threshold.



of mPFC and conflict in modulation of decision threshold ( $P = 0.23$ ), affected individuals in ON DBS sessions showed the opposite relationship, differing from both control individuals ( $P = 0.03$ ) and OFF DBS sessions ( $P = 0.014$ ).

Finally, we examined how the estimated change in decision threshold translates into response time distributions (Fig. 3c). Higher theta/threshold was associated with more dispersed response time distributions and a lower probability of fast suboptimal choices. These Bayesian DDM parameter fits were corroborated by full DDM (non-hierarchical) analysis using the fast-dm program<sup>21</sup> (Supplementary Results and Supplementary Fig. 4).

### Study II: intraoperative direct recording of the STN

With a nearly identical task, we tested individuals with Parkinson's disease during DBS implantation. The subjects first performed the task 3–5 h before their surgical session, and again during surgery for DBS implantation when STN area activity was recorded. In the pre-surgical session, participants performed above chance on the training phase ( $t_7 = 6.74$ ,  $P = 0.001$ , mean = 68% accurate, s.d. = 8%), demonstrating that the task was well-learned before surgery. Participants performed less well during surgery (M = 58% accurate, s.d. = 21%; this was not significantly different, paired samples  $t$  test,  $P = 0.12$ ), likely as a result of the distraction and stress of the surgical environment (Supplementary Fig. 5).

Intracranial EEG recordings revealed low-frequency power enhancement and beta power suppression in the STN area (Fig. 4). High-conflict conditions were specifically

characterized by a rapid diminishment in low-frequency power, followed by greater cue-locked high-delta power (2.5 to 4 Hz) approximately 750 ms after stimulus presentation in the dorsal STN electrodes, as well as greater post-response power (3–5 Hz) across all electrodes. These findings provide evidence that decision conflict is reflected in local STN area activity during the same period as those observed in mPFC and, notably, with similar time courses as those observed in monkey single-unit recordings<sup>11</sup>. Similar effects were seen in both win-win and lose-lose conditions (Supplementary Fig. 6), and in a *post-hoc* analysis of a subgroup of the best performers (Supplementary Fig. 7). Together with the results of study I, these findings are consistent with the suggestion that mPFC and STN communicate in low-frequency bands to represent decision conflict and that STN-DBS interferes with the normal ability of the STN to react to decision conflict (that is, by modulating decision threshold).

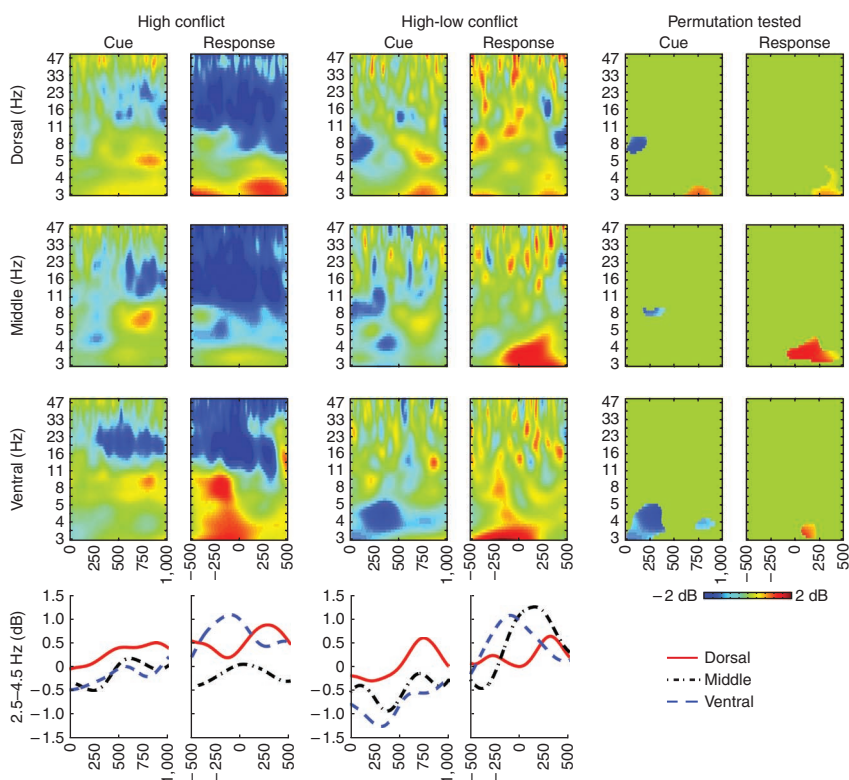


**Figure 4** Intracranial EEG from the STN for dorsal, middle and ventral leads. Both beta suppression and theta enhancement were observed in the STN. The rightmost columns show the condition-wide differences revealed by permutation testing. High-conflict trials were characterized by a diminishment of low-frequency power across leads, greater post-cue activity in the dorsal lead and greater post-response activity across leads. The bottom row shows intracranial EEG data filtered from 2.5–4.5 Hz.

## DISCUSSION

Direct manipulation of and recording from the STN yielded electrophysiological evidence for mPFC-STN interactions during conflict-instantiated control. Cognitive systems involved in evaluating stimuli and adapting actions are known to be instantiated in cortico-striatal circuits, including mPFC and STN<sup>5,7,10,11,15,17,18,22,23</sup>. High-frequency STN-DBS has been proposed to compromise the dynamic functioning and self-regulation of this system, leading to impulsive or poorly planned behaviors<sup>5,15</sup>. Our results identify a potential mechanistic role of low-frequency band dynamics for instantiating conflict-specific communication in this network.

In particular, we found that mPFC activity predicted an increase in the decision threshold during high-conflict trials and that STN-DBS reversed this relationship: high mPFC theta was associated with a speeding of response times and reduction of decision threshold. This inverse relationship between conflict and response time resulting from STN-DBS has been previously described for high-conflict win-win trials in which multiple high-value responses result in impulsive responding<sup>5</sup>. Given the hypothesis that mPFC and STN interact to unidirectionally increase decision threshold<sup>6–9</sup>, this finding may seem surprising. However, an a priori computational explanation<sup>15</sup> of the pattern of response time and accuracy findings that we observed suggests that, by disrupting the mPFC-STN route, DBS may reveal the influence of parallel cortico-striatal mechanisms for facilitating high-value actions and reducing decision thresholds<sup>23–25</sup>.

Simulations with the DDM have shown that, during reinforcement-based decisions, thresholds are raised as a function of conflict in both neural models of basal ganglia and healthy human participants (R. Ratcliff and M. Frank, unpublished data). We found that this effect is related to increases in mPFC theta in both healthy control and affected individuals in OFF DBS sessions, and that DBS interferes with this relationship. The specificity of behavioral findings and replication across studies<sup>15</sup> suggest that high-conflict suboptimal choices in affected individuals in ON DBS sessions are likely to result from premature responses. Our results extend these findings, demonstrating that this effect may be mediated by mPFC-STN interactions, as formalized in terms of decision threshold. Although field spread and antidromic stimulation of the cortex are possible side effects of STN-DBS, the observation that reinforcement conflict is reflected in the STN area partially mitigates this potential interpretative issue. Monkey electrophysiological recording data also support this interpretation, in that mPFC and STN unit activity have been associated with behavioral inhibition during controlled responding with short latencies from mPFC to STN<sup>10,11</sup>.

Alternatively, it is possible that mPFC-STN interactions are mediated indirectly, via mPFC effects on the inferior frontal gyrus (IFG), which then inhibits behavior via STN. Indeed, diffusion tensor imaging studies suggest that both mPFC and IFG project directly to STN<sup>7</sup>. Combined transcranial magnetic stimulation and functional connectivity studies imply that, although mPFC is necessary for behavioral inhibition, its effects are mediated via projections to IFG and then STN<sup>13</sup>. Other neuroimaging findings suggest that decision threshold is modulated by functional connectivity between mPFC and striatum, rather than by STN<sup>23,24</sup>. However, these data are not mutually exclusive; although our results suggest that the STN is involved in dynamically raising the threshold as a function of reinforcement and decision conflict, other studies have focused on the role of mPFC-striatal communication in reducing decision threshold in a speed-over-accuracy tradeoff<sup>23,24</sup>. In fact, this type of cortico-striatal effect is posited to cause the win-win speeding observed in affected individuals in ON DBS sessions, which is otherwise counteracted by intact STN conflict processing<sup>15</sup> (also see **Supplementary Discussion**).

Systems-level neural models of cortical-basal ganglia interactions suggest that both STN and striatum exert modulatory effects that would be reflected in a change in decision threshold, with different underlying mechanisms<sup>5,25</sup>. Some algorithmic models also posit that response conflict is computed in the STN, and in the simple case of two responses, cortical-basal ganglia circuitry precisely implements the diffusion decision process<sup>22</sup>. Although broadly consistent with the neural models mentioned above and our data, this formulation suggests a particular form of the function of conflict encoded by the STN, proportional to the sum of the evidence across responses<sup>22</sup>. This function implies that STN activity would be greatest in win-win, lowest in lose-lose and intermediate in our low-conflict win-lose condition. Instead, our intraoperative recording data suggest that conflict is processed as a function of similarity of the two response options (see **Supplementary Fig. 6**). Notably, this parallels an influential theory of the representation of conflict in mPFC<sup>3</sup>, especially in regard to EEG signals<sup>4</sup>.

Consistent with previous findings, mPFC theta power (4–8 Hz) enhancement was present during both low-conflict and high-conflict trials, but it was only during high-conflict situations that it was behaviorally relevant<sup>17–19</sup>. Activity in these low-frequency bands may reflect a neural substrate for cortico-basal ganglia communication during conflict-related behavioral adjustment. It is notable that decision conflict reflected in the STN area is in the same broad ~2.5–5-Hz range as is the frequency of Parkinson's tremor and associated oscillations in the STN<sup>26,27</sup>. Models also exhibit slow STN oscillatory activity in the dopamine-depleted state<sup>5,28</sup>, which are exacerbated with increased cortical conflict<sup>5</sup>. Although speculative, this model predicts that higher amplitude tremor may be detectable when affected individuals are faced with increased decision conflict.

In summary, we found that STN-DBS dynamically altered the coupling between low-frequency cortical signals and conflict-related behavioral adaptation. Bayesian parameter estimation using the drift diffusion model confirmed that this is a result of a disruption of an mPFC-STN network that raises decision threshold following the evaluation of conflict. Alteration of this network facilitated conflict-induced speeding, suggesting an interactive cortico-basal ganglia mechanism by which STN-DBS induces impulsivity<sup>14</sup>. In addition, intraoperative recordings demonstrated that the STN area is characterized by enhanced low-frequency activity during learned high conflict situations. We conclude that the STN is important for buying time for cortico-striatal systems to react and respond to conflict. Thus, future research on DBS protocols may benefit from an attempt to preserve this low frequency communication between mPFC and STN, to mitigate cognitive and impulsivity side effects associated with DBS<sup>14,15,29</sup>.

## METHODS

Methods and any associated references are available in the online version of the paper at <http://www.nature.com/natureneuroscience/>.

*Note: Supplementary information is available on the Nature Neuroscience website.*

## ACKNOWLEDGMENTS

The authors express their gratitude to T. Norton and his surgical staff for their support during the intraoperative recording sessions, L. Trujillo for a review of permutation methods, E.J. Wagenmakers for consultation on Bayesian data analysis, J.J.B. Allen and E.F. Martino for laboratory resources that facilitated some data acquisition and analyses, and K. Carlisle for help with subject recruitment. This project was funded by a grant from the Michael J. Fox Foundation to M.J.F.

## AUTHOR CONTRIBUTIONS

M.J.F., J.F.C. and M.X.C. designed the experiments. J.F.C., C.M.F., J.S. and S.J.S. recruited and ran participants. J.F.C. and M.X.C. processed the EEG data. T.V.W. and M.J.F. designed the computational models. J.F.C. and M.J.F. wrote the manuscript.

## COMPETING FINANCIAL INTERESTS

The authors declare no competing financial interests.

Published online at <http://www.nature.com/natureneuroscience/>.

Reprints and permissions information is available online at <http://www.nature.com/reprints/index.html>.

1. Miller, E.K. The prefrontal cortex and cognitive control. *Nat. Rev. Neurosci.* **1**, 59–65 (2000).
2. Miller, E.K. & Cohen, J.D. An integrative theory of prefrontal cortex function. *Annu. Rev. Neurosci.* **24**, 167–202 (2001).
3. Botvinick, M.M., Braver, T.S., Barch, D.M., Carter, C.S. & Cohen, J.D. Conflict monitoring and cognitive control. *Psychol. Rev.* **108**, 624–652 (2001).
4. Yeung, N., Botvinick, M.M. & Cohen, J.D. The neural basis of error detection: conflict monitoring and the error-related negativity. *Psychol. Rev.* **111**, 931–959 (2004).
5. Frank, M.J. Hold your horses: a dynamic computational role for the subthalamic nucleus in decision making. *Neural Netw.* **19**, 1120–1136 (2006).
6. Nambu, A., Tokuno, H. & Takada, M. Functional significance of the cortico-subthalamo-pallidal 'hyperdirect' pathway. *Neurosci. Res.* **43**, 111–117 (2002).
7. Aron, A.R., Behrens, T.E., Smith, S., Frank, M.J. & Poldrack, R.A. Triangulating a cognitive control network using diffusion-weighted magnetic resonance imaging (MRI) and functional MRI. *J. Neurosci.* **27**, 3743–3752 (2007).
8. Inase, M., Tokuno, H., Nambu, A., Akazawa, T. & Takada, M. Corticostriatal and cortico-subthalamo input zones from the presupplementary motor area in the macaque monkey: comparison with the input zones from the supplementary motor area. *Brain Res.* **833**, 191–201 (1999).
9. Takada, M. *et al.* Organization of inputs from cingulate motor areas to basal ganglia in macaque monkey. *Eur. J. Neurosci.* **14**, 1633–1650 (2001).
10. Isoda, M. & Hikosaka, O. Switching from automatic to controlled action by monkey medial frontal cortex. *Nat. Neurosci.* **10**, 240–248 (2007).
11. Isoda, M. & Hikosaka, O. Role for subthalamic nucleus neurons in switching from automatic to controlled eye movement. *J. Neurosci.* **28**, 7209–7218 (2008).
12. Fleming, S.M., Thomas, C.L. & Dolan, R.J. Overcoming status quo bias in the human brain. *Proc. Natl. Acad. Sci. USA* **107**, 6005–6009 (2010).
13. Neubert, F.X., Mars, R.B., Buch, E.R., Olivier, E. & Rushworth, M.F. Cortical and subcortical interactions during action reprogramming and their related white matter pathways. *Proc. Natl. Acad. Sci. USA* **107**, 13240–13245 (2010).
14. Hälbig, T.D. *et al.* Subthalamic deep brain stimulation and impulse control in Parkinson's disease. *Eur. J. Neurol.* **16**, 493–497 (2009).
15. Frank, M.J., Samanta, J., Moustafa, A.A. & Sherman, S.J. Hold your horses: impulsivity, deep brain stimulation, and medication in parkinsonism. *Science* **318**, 1309–1312 (2007).
16. Ratcliff, R. & McKoon, G. The diffusion decision model: theory and data for two-choice decision tasks. *Neural Comput.* **20**, 873–922 (2008).
17. Cavanagh, J.F., Cohen, M.X. & Allen, J.J. Prelude to and resolution of an error: EEG phase synchrony reveals cognitive control dynamics during action monitoring. *J. Neurosci.* **29**, 98–105 (2009).
18. Cavanagh, J.F., Frank, M.J., Klein, T.J. & Allen, J.J.B. Frontal theta links prediction errors to behavioral adaptation in reinforcement learning. *Neuroimage* **49**, 3198–3209 (2010).
19. Cohen, M.X. & Cavanagh, J.F. Single-trial regression elucidates the role of prefrontal theta oscillations in response conflict. *Front. Psychol.* **2**, 1–12 (2011).
20. Hanslmayr, S. *et al.* The electrophysiological dynamics of interference during the Stroop task. *J. Cogn. Neurosci.* **20**, 215–225 (2008).
21. Voss, A. & Voss, J. A fast numerical algorithm for the estimation of diffusion-model parameters. *J. Math. Psychol.* **52**, 1–9 (2008).
22. Bogacz, R. & Gurney, K. The basal ganglia and cortex implement optimal decision making between alternative actions. *Neural Comput.* **19**, 442–477 (2007).
23. Forstmann, B.U. *et al.* Striatum and pre-SMA facilitate decision-making under time pressure. *Proc. Natl. Acad. Sci. USA* **105**, 17538–17542 (2008).
24. Forstmann, B.U. *et al.* Cortico-striatal connections predict control over speed and accuracy in perceptual decision making. *Proc. Natl. Acad. Sci. USA* **107**, 15916–15920 (2010).
25. Lo, C.C. & Wang, X.J. Cortico-basal ganglia circuit mechanism for a decision threshold in reaction time tasks. *Nat. Neurosci.* **9**, 956–963 (2006).
26. Hutchison, W.D. *et al.* Neurophysiological identification of the subthalamic nucleus in surgery for Parkinson's disease. *Ann. Neurol.* **44**, 622–628 (1998).
27. Tass, P. *et al.* The causal relationship between subcortical local field potential oscillations and Parkinsonian resting tremor. *J. Neural Eng.* **7**, 16009 (2010).
28. Humphries, M.D., Stewart, R.D. & Gurney, K.N. A physiologically plausible model of action selection and oscillatory activity in the basal ganglia. *J. Neurosci.* **26**, 12921–12942 (2006).
29. Thobois, S. *et al.* STN stimulation alters pallidal-frontal coupling during response selection under competition. *J. Cereb. Blood Flow Metab.* **27**, 1173–1184 (2007).

## ONLINE METHODS

**Study I: OFF versus ON STN-DBS.** Subjects were referred to the study by their healthcare provider based on an assessment of eligibility. Inclusion criterion included a diagnosis of mild to moderate idiopathic Parkinson's disease as assessed by their physician, being over 40 years old, being medically stable for 3 months after DBS surgery and their referring neurologist determining that they could tolerate a period with the DBS unit turned off in a preliminary screening, absence of a significant medical history not related directly to Parkinson's disease (for example, stroke, head injury, clinical dementia, epilepsy, life-threatening concurrent illness such as schizophrenia or manic depression, documented or suspected history of drug abuse and/or alcoholism), and the presence of at least two of the following three symptoms: resting tremor, rigidity and bradykinesia. All of the subjects gave informed consent and were compensated \$25 for their participation. We tested 19 individuals with Parkinson's disease in both the ON and OFF DBS conditions. The research ethics committee of the University of Arizona approved these experiments. Two individuals were unable to tolerate the DBS stimulator being turned off and were sent home before completing the experiment. Computer problems corrupted the data from another participant. Two participants failed to learn the task according to criterion described below. The final sample for EEG and behavioral data were taken from the remaining 14 participants (**Supplementary Table 4**). Details of the control group participants can be found in the **Supplementary Results**.

The task consisted of a series of brief forced-choice training blocks with 16 trials, each followed by a subsequent testing block with 16 trials (**Fig. 1b**). There were eight train/test blocks, with an optional additional two train/test blocks per set that were performed if the participants agreed. Participants performed these sets twice, once in the ON DBS and once in the OFF DBS condition, in a randomized counterbalanced order. There was always a 30-min break between the time that the stimulator was turned on or off and the beginning of each task. Stimulus pictures were not repeated between blocks during the experiment, and the association between any specific picture and training block / reward value was randomized between participants. Most participants completed the maximum ten blocks in each DBS condition (11 of 14 ON, 13 of 14 OFF); the others completed eight blocks.

**Study I: EEG recording and processing.** Scalp voltage was measured using 62 Ag/AgCl electrodes referenced to a site immediately posterior to Cz using a Synamps<sup>2</sup> system (bandpass filter 0.5–100 Hz, 1,000-Hz sampling rate). During pre-processing, data were low-pass filtered at 50 Hz and eyeblinks were removed using independent components analysis<sup>30</sup>. The 50-Hz low-pass temporal filter effectively removed the majority of the DBS artifact in the ON condition. Epochs were transformed to current source density<sup>31</sup>, which acts as a spatial filter by computing the second spatial derivative of voltage between nearby electrode sites. Data from the FCz electrode were used for display and analysis.

Time-frequency calculations were computed using custom-written Matlab (MathWorks) routines<sup>17–19</sup>. Time-frequency measures were computed by multiplying the fast Fourier transformed (FFT) power spectrum of single trial EEG data with the FFT power spectrum of a set of complex Morlet wavelets, and taking the inverse FFT. The wavelet family is defined as a set of Gaussian-windowed complex sine waves,  $e^{-i2\pi ft} e^{-t^2/(2\sigma^2)}$ , where  $t$  is time,  $f$  is frequency (which increased from 2.5 to 50 Hz in 50 logarithmically spaced steps) and  $\sigma$  defines the width (or number of cycles) of each frequency band, set according to  $4.5/(2\pi f)$ . The end result of this process is identical to time-domain signal convolution. Power was defined as  $Z(t)$  (power time series:  $p(t) = \text{real}[z(t)]^2 + \text{imag}[z(t)]^2$ ), and was normalized by conversion to a decibel scale ( $10 \log_{10}[\text{power}(t)/\text{power}(\text{baseline})]$ ), allowing a direct comparison of effects across frequency bands. Values for statistical analysis were summed (to get total area under the curve) over time and frequency (cue-locked, 350–550 ms, 4–8 Hz). For single-trial analyses, power was taken from the Hilbert transform of filtered (4–8 Hz) single-trial EEG. Epochs were baseline corrected for each frequency by the average power from –300 to –200 ms before the onset of the stimulus.

**Study I: statistical analyses and DDM.** Two participants were removed from all analyses for failing to learn any blocks during one of the ON or OFF sessions, set according to a criterion of >50% accuracy in each of the AB and CD sets by the end of each block. Statistical tests for DBS differences in EEG theta power were performed on difference scores (high – low conflict) to highlight

conflict-specific EEG events while controlling for global effects resulting from STN-DBS. Statistical tests of the single-trial relationship between cue-locked theta power and immediate response time were calculated as individual regression weights.

Estimation of the underlying decision-making process was accomplished by DDM analysis<sup>16</sup> of test phase choices (after learning). The DDM models two-choice decision making as a noisy process accumulating evidence over time. Although the noisy accumulation of evidence is most transparently applied in tasks involving noise in the stimulus, the same process describes noise in neural processing for static stimuli, and in value-based decision making accounts for dynamic shifts in attention from one option to the other<sup>32</sup>. This process approaches one of two boundaries with a certain speed (drift-rate, influenced by the amount of evidence conveyed by the stimuli). When one of the two boundaries is crossed, the associated response is executed. The distance between the two boundaries is called the decision threshold; larger thresholds lead to slower, but more accurate, responding, as the influence of noise in the accumulation of evidence is reduced, whereas smaller thresholds lead to faster, more impulsive responding with increased error probability. Inter-trial variability in drift and non-decision time were estimated as well (see **Supplementary Results**); simulations without these variability parameters provided a worse fit to the data, but led to similar results).

Hierarchical Bayesian parameter estimation using Markov-chain Monte-Carlo was used to estimate posterior distributions of the DDM parameters<sup>33,34</sup>. This Bayesian form of analysis allows simultaneous estimation of model parameters for the whole group, which constrains estimation of parameters for each individual participant. There were 30,000 samples generated from the posteriors; the first 10,000 (burn-in) and every second (thinning) were discarded. Proper chain convergence was tested by comparing between-chain and inter-chain variance<sup>35</sup>.

On the basis of prior theoretical work<sup>36</sup>, DBS and theta power were predicted to have an effect on decision threshold while also allowing for different levels of difficulty to influence drift rate (evidence accumulation). Thus, although all parameters including threshold were estimated from the DDM likelihood functions translating response time distributions and error rates to the underlying generative parameters, we also estimated the effects of other observable variables on this threshold in the same hierarchical framework,  $\text{threshold} = a + e_{\text{DBS}} \times \text{DBS}_{\text{status}} + e_{\theta} \times \theta + e_{\text{interaction}} \times \text{DBS}_{\text{status}} \times \theta$ , with  $a$  reflecting the intercept,  $\text{DBS}_{\text{status}}$  reflecting ON or OFF, and  $\theta$  reflecting the single trial-estimated theta-band activity (the same EEG data used in the individual regression weights in **Fig. 2c**). The coefficients  $e_{\text{DBS}}$ ,  $e_{\theta}$  and  $e_{\text{interaction}}$  provide weights to test the effect of DBS on decision threshold (for average  $\theta$  power), the effect of  $\theta$  on decision threshold, and the interaction of  $\theta$  and DBS on decision threshold. The theta and interaction terms were estimated separately for low-conflict and high-conflict trials. To ensure these effects were independent of trial-type effects on drift rate, we estimated drift rates separately. To further test the specificity of the findings, we constructed alternative models in which drift rate rather than threshold varied as a function of  $\theta$  and DBS; these models provided a worse fit to the data and did not yield significant associations.

Bayesian hypothesis testing was performed by analyzing the probability mass of the parameter region in question (estimated by the number of samples drawn from the posterior that fall in this region; for example, percentage of posterior samples smaller than zero). This leads to a direct probability measure denoted  $P$  that can be interpreted in a similar way, but is not equivalent, to  $P$  values as estimated by frequentist methods. Additional analysis using the Bayes factor and deviance information criterion can be found in the **Supplementary Results**.

**Study II: intraoperative recording of the STN.** Eight participants with Parkinson's disease consented to participate. The research ethics committee of the University of Arizona approved the study and all participants gave informed consent. One participant reported here performed both the intraoperative procedure and the ON/OFF study. Participant demographics are shown in **Supplementary Table 5**.

The task was very similar to the task used for Study I except that there were always four train/test blocks, stimuli consisted of simple colored shapes, and there were a total of 34 low-conflict and 68 high-conflict (34 win-win and 34 lose-lose) test trials for each task. Participants first performed the task in their hospital waiting room 3–5 h before the surgery to become familiarized with the instructions and response demands. Performance data from these two sessions (pre-surgery, surgery) are shown in **Supplementary Figure 5**.

**Study II: intracranial EEG recording and processing.** Intracranial EEG was recorded from a Medtronic 3387 stimulating electrode in the left STN using a Synamps<sup>2</sup> system (bandpass filter 0.05–500 Hz, 2,000-Hz sampling rate) referenced to a mastoid site and grounded on the collarbone. Electrode placement was determined by the surgical staff based on pre-operative stereotaxic planning, the firing pattern from the microelectrode recordings, and immediate clinical effectiveness of stimulation. The surgical team sought to place the quadripolar electrode so that the distal (ventral) contact corresponded to the ventral boundary of the STN as determined by microelectrode recordings. The Medtronic electrode included four contacts, which were bipolar referenced resulting in three separate recordings of STN area activity. These recordings are referred to by their proximal location to each other: ventral, middle and dorsal, although their exact location in regard to subnuclei of the STN is unknown.

Time-frequency calculations were identical to those used in study I. Permutation tests were performed on the voltage difference between high- and low-conflict conditions using custom-written Matlab routines. This process tests the null hypothesis that the data in the high and low conflict conditions are interchangeable. First, paired sample *t* tests were computed at each time-frequency point (pixel) of the empirical data. These tests were then re-done 5,000 times with data randomly shuffled between high and low conflict conditions within each participant. Each permutation used conditions with the same number of epochs (by randomly selecting from the pool of the larger set) in order to control for unequal weightings of evidence. Multiple comparison correction was done using

weighted cluster-based thresholding, sometimes known as exceedance mass<sup>37</sup>. The sum of the *t* values in each cluster of significant voxels in the empirical data was thresholded to be larger than 97.5% of permuted significant clusters (separately for positive and negative *t* value clusters), providing a two-tailed 5% level of family-wise error control of multiple comparisons. This method provides a data-driven hypothesis test that identifies where conditions differ over time-frequency space.

30. Delorme, A. & Makeig, S. EEGLAB: an open source toolbox for analysis of single-trial EEG dynamics including independent component analysis. *J. Neurosci. Methods* **134**, 9–21 (2004).
31. Kayser, J. & Tenke, C.E. Principal components analysis of Laplacian waveforms as a generic method for identifying ERP generator patterns. I. Evaluation with auditory oddball tasks. *Clin. Neurophysiol.* **117**, 348–368 (2006).
32. Krajbich, I., Armel, C. & Rangel, A. Visual fixations and the computation and comparison of value in simple choice. *Nat. Neurosci.* **13**, 1292–1298 (2010).
33. Lee, M.D., Fuss, I. & Navarro, D.J. in *Advances in Neural Information Processing Systems* (eds. B. Scholkopf, J. Platt & T. Hoffman) 809–815 (MIT Press, Cambridge, Massachusetts, 2007).
34. Vandekerckhove, J., Tuerlinckx, F. & Lee, M.D. Hierarchical diffusion models for two-choice response time. *Psychol. Methods* **16**, 44–62 (2011).
35. Gelman, A. *Bayesian Data Analysis* 2nd edn. (Chapman & Hall/CRC, 2004).
36. Frank, M.J. & Claus, E.D. Anatomy of a decision: striato-orbitofrontal interactions in reinforcement learning, decision making, and reversal. *Psychol. Rev.* **113**, 300–326 (2006).
37. Nichols, T.E. & Holmes, A.P. Nonparametric permutation tests for functional neuroimaging: a primer with examples. *Hum. Brain Mapp.* **15**, 1–25 (2002).